



Supplement of

Interannual variability of summertime cross-isobath exchanges in the northern South China Sea: ENSO and riverine influences

Yunping Song et al.

Correspondence to: Zhiqiang Liu (liuzq@sustech.edu.cn) and Zhongya Cai (zycai@um.edu.mo)

The copyright of individual parts of the supplement might differ from the article licence.

The large-runoff years are identified by a simple percentile rule: for each year we compute the summer-mean Pearl River discharge $Q(y)$, and label years with $Q(y) \geq Q_{70\%}$ as high-runoff. Over 2000–2022, this threshold equals $26,000 \text{ m}^3 \text{ s}^{-1}$. Figure S1 shows that raising the cutoff to $Q_{80\%}$ produces almost the same spatial patterns with only minor amplitude differences, which confirms that $Q_{70\%}$ is sufficient to distinguish between large- and low-runoff years.

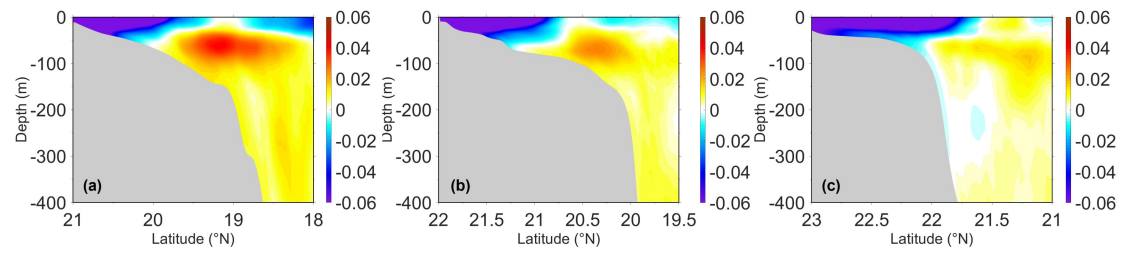


Figure S1. (a) Salinity anomaly profiles (psu) during summer in years exceeding the 80% runoff threshold (Table 2) at Transect A; (b) salinity anomaly profiles during summer in years exceeding the 80% runoff threshold at Transect B; (c) salinity anomaly profiles during summer in years exceeding the 80% runoff threshold at Transect C.

The simple conditional-average maps compared to Fig. 4c, d are shown in Fig. S2. The resulting composites over the years of the positive MVPC1 phase appear consistent with the regression method we employed, differing only in minor details. Consequently, we retain the regression maps in the main text.

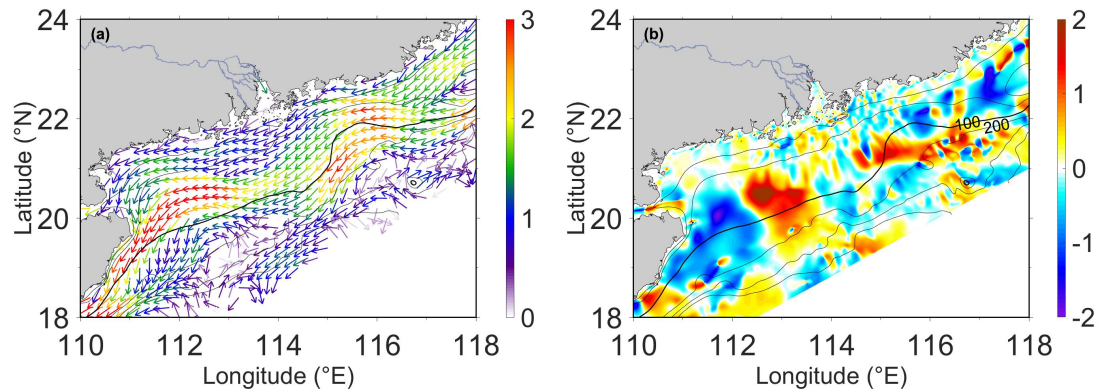


Figure S2. (a) Mean velocity vector anomalies (cm s^{-1}), and (b) mean cross-isobath velocity anomalies (cm s^{-1}) during summer in positive MVPC1 years (Table 1).

The spatial structure of the cross-isobath velocity anomaly contributed by the term GMF during

positive MVPC1 years is displayed in Fig. S3. Its magnitude is negligible compared with the other terms (except within the PRE, which is away from the studied NSCS shelf). Therefore, it is reasonable for us to omit the discussion of this item in the main text.

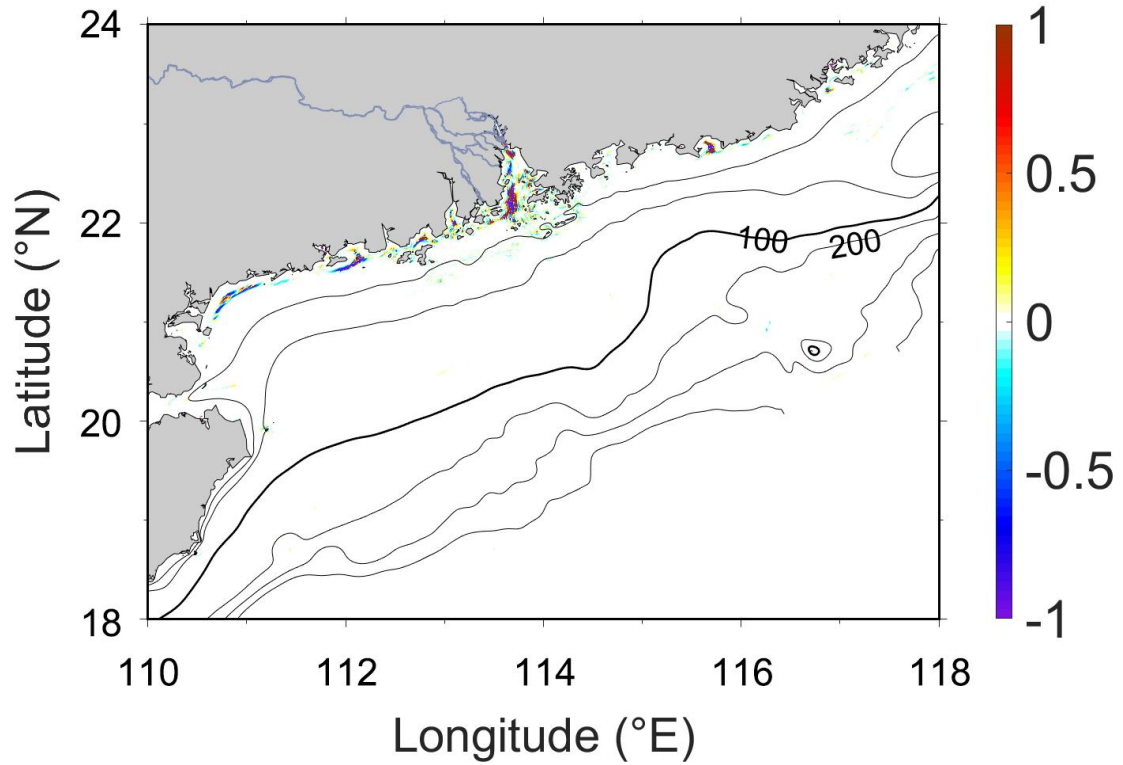


Figure S3. Regression maps of horizontal cross-isobath velocity anomalies (cm s^{-1}) during positive MVPC1 years (Table 1), attributed to the gradient of momentum flux (GMF).

Figures S4 and S5 illustrate the situation during negative MVPC1 (La Niña) years, which are essentially mirror images of the positive phase. Although we only present the along-isobath distribution of density and buoyancy frequency squared anomalies in the main text, cross-isobath profiles such as those in Fig. S6 are non-negligible for capturing the total JEBAR anomaly; when combined and taking the topographical factors into account, they yield a similar structure as Fig. 6a during positive MVPC1 years (and its opposite in negative years).

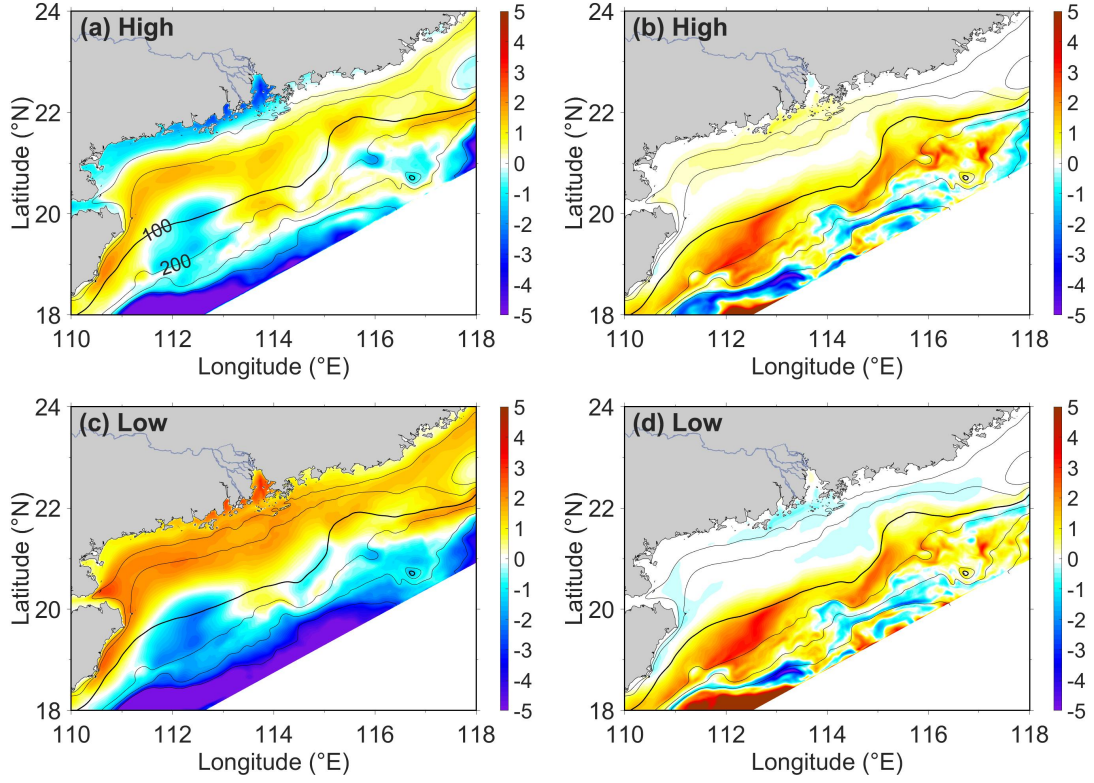


Figure S4. Regression maps of horizontal components ($\text{m}^2 \text{s}^{-2}$) in the JEBAR term during the summer of negative MVPC1 years, under different runoff conditions: (a, b) correspond to positive PC1 years, and (c, d) to negative PC1 years. Panels show (a, c) the full baroclinic gradient term ($\frac{g}{\rho_0} \int_{-H}^0 z(\rho - \bar{\rho}) dz$) and (b, d) the contribution from vertical density stratification ($-\frac{g}{\rho_0} \int_{-H}^0 \frac{z^2}{2} \frac{\partial(\rho - \bar{\rho})}{\partial z} dz$). The MVPC1 time series is shown in Fig. 3g, with corresponding positive-phase years listed in Table 1, while the PC1 time series is shown in Fig. 3h with its positive-phase years listed in Table 2. The two-stage regression approach is detailed in Section 3.2.

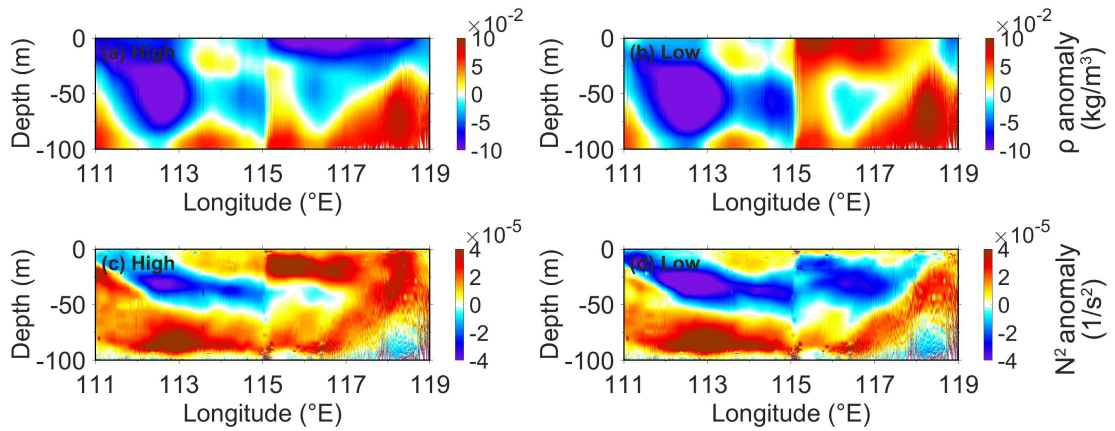


Figure S5. Regression maps of hydrographic anomaly profiles along the 100 m isobath during the summer of negative MVPC1 years (Table 1), under different runoff conditions: (a, c) correspond to positive PC1 years, and (b, d) to negative PC1 years (Table 2). Panels show (a, b) density anomalies

(kg m^{-3}) and (c, d) buoyancy frequency squared anomalies (s^{-2}). The two-stage regression approach is detailed in Section 3.2.

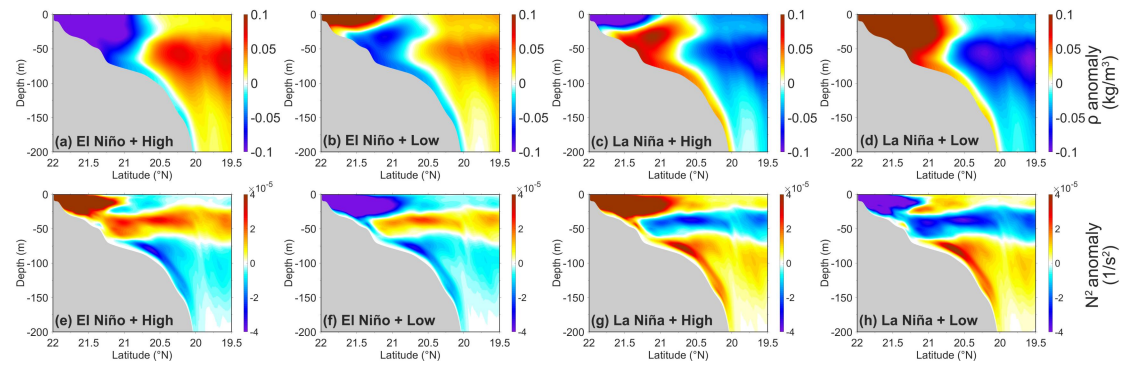


Figure S6. Regression maps of hydrographic anomaly profiles at Transect B under different climate and runoff conditions. Panels (a–d) show density anomalies (kg m^{-3}), and panels (e–h) show buoyancy frequency squared anomalies (s^{-2}). Results correspond to: (a, b, e, f) positive MVPC1 years (Table 1) and (c, d, g, h) negative MVPC1 years; with (a, c, e, g) representing positive PC1 years and (b, d, f, h) negative PC1 years (Table 2). The two-stage regression approach is detailed in Section 3.2.